chemoselective glycoblotting and MALDI-TOF/TOF mass spectrometry. Angew Chem Int Ed Engl 2004;44:91-96.
22. Furukawa J, Shinohara Y, Kuramoto H, Miura Y, Shimaoka H, Kurogochi M, et al. Comprehensive approach to structural and functional glycomics based on chemoselective glycoblotting and sequential tag conversion. Anal Chem 2008;80:1094-1101.
23. Ichida F, Tsuji T, Omata M, Ichida T, Inoue K, Kamimura T, et al. New Inuyama Classification; new criteria for histlogical assessment of chronic hepatitis. Int Hepatol Commun 1996;6:112-119.
24. The Liver Study Group of Japan. The general rules for the clinical and pathological study of primary liver cancer. 3rd English ed. Tokyo, Japan: Kanehara & Co.
25. Akaike H. A new look at the statistical model identification. IEEE Trans Autom Control 1974;19:716-723.
26. Nomura F, Ohnishi K, Tanabe Y. Clinical features and prognosis of hepatocellular carcinoma with reference to serum alpha-fetoprotein levels. Analysis of 606 patients. Cancer 1989;64:1700-1707.
27. Hanazaki K, Kajikawa S, Koide N, Adachi W, Amano J. Prognostic factors after hepatic resection for hepatocellular carcinoma with hepatitis C viral infection: univariate and multivariate analysis. Am J Gastroenterol 2001;96:1243-1250.
28. Matsumoto Y, Suzuki T, Asada I, Ozawa K, Tobe T, Honjo I. Clinical classification of hepatoma in Japan according to serial changes in serum alpha-fetoprotein levels. Cancer 1982;49:354-360.
29. Yang X, Zhang Y, Zhang L, Mao J. Silencing alpha-fetoprotein expression induces growth arrest and apoptosis in human hepatocellular cancer cell. Cancer Lett 2008;271:281-293.
30. Mizejewski GJ. Alpha-fetoprotein structure and function: relevance to isoforms, epitopes, and conformational variants. Exp Biol Med (Maywood) 2001;226:377-408.
31. Smith JB. Occurrence of alpha-fetoprotein in acute viral hepatitis. Int J Cancer 1971;8:421-424.
32. Silver HK, Gold P, Shuster J, Javitt NB, Freedman SO, Finlayson ND. Alpha(1)-fetoprotein in chronic liver disease. N Engl J Med 1974;291:506-508.
33. Fujiyama S, Tanaka M, Maeda S, Ashihara H, Hirata R, Tomita K. Tumor markers in early diagnosis, follow-up and management of patients with hepatocellular carcinoma. Oncology 2002;62(Suppl 1):57-63.
34. Kudo T, Nakagawa H, Takahashi M, Hamaguchi J, Kamiyama N, Yokoo H, et al. N-glycan alterations are associated with drug resistance in human hepatocellular carcinoma. Mol Cancer 2007;6:32.
35. Tang Z, Varghese RS, Bekesova S, Loffredo CA, Hamid MA, Kyselova Z, et al. Identification of N-glycan serum markers associated with hepatocellular carcinoma from mass spectrometry data. J Proteome Res 2010;9:104-112.
36. Ding N, Nie H, Sun X, Sun W, Qu Y, Liu X, et al. Human serum N-glycan profiles are age and sex dependent. Age Ageing 2011;40:568-575.

miR-1290 and its potential targets are associated with characteristics of estrogen receptor α-positive breast cancer

Yumi Endo[1], Tatsuya Toyama[1], Satoru Takahashi[2], Nobuyasu Yoshimoto[1], Mai Iwasa[1], Tomoko Asano[1], Yoshitaka Fujii[1] and Hiroko Yamashita[1]

Departments of [1]Oncology, Immunology and Surgery [2]Experimental Pathology and Tumor Biology, Nagoya City University Graduate School of Medical Sciences, 1 Kawasumi, Mizuho-cho, Mizuho-ku, Nagoya 467-8601, Japan

H Yamashita is now at Breast and Endocrine Surgery, Hokkaido University Hospital, Kita 14, Nishi 5, Sapporo 060-8648, Japan

Correspondence should be addressed to H Yamashita
Email
hirokoy@huhp.hokudai.ac.jp

Endocrine-Related Cancer

Abstract

Recent analyses have identified heterogeneity in estrogen receptor α (ERα)-positive breast cancer. Subtypes called luminal A and luminal B have been identified, and the tumor characteristics, such as response to endocrine therapy and prognosis, are different in these subtypes. However, little is known about how the biological characteristics of ER-positive breast cancer are determined. In this study, expression profiles of microRNAs (miRNAs) and mRNAs in ER-positive breast cancer tissue were compared between ER^{high} $Ki67^{low}$ tumors and ER^{low} $Ki67^{high}$ tumors by miRNA and mRNA microarrays. Unsupervised hierarchical clustering analyses revealed distinct expression patterns of miRNAs and mRNAs in these groups. We identified a downregulation of miR-1290 in ER^{high} $Ki67^{low}$ tumors. Among 11 miRNAs that were upregulated in ER^{high} $Ki67^{low}$ tumors, quantitative RT-PCR detection analysis using 64 samples of frozen breast cancer tissue identified six miRNAs (let-7a, miR-15a, miR-26a, miR-34a, miR-193b, and miR-342-3p). We picked up 11 genes that were potential target genes of the selected miRNAs and that were differentially expressed in ER^{high} $Ki67^{low}$ tumors and ER^{low} $Ki67^{high}$ tumors. Protein expression patterns of the selected target genes were analyzed in 256 ER-positive breast cancer samples by immunohistochemistry: miR-1290 and its putative targets, *BCL2*, *FOXA1*, *MAPT*, and *NAT1*, were identified. Transfection experiments revealed that introduction of miR-1290 into ER-positive breast cancer cells decreased expression of NAT1 and FOXA1. Our results suggest that miR-1290 and its potential targets might be associated with characteristics of ER-positive breast cancer.

Key Words
- breast cancer
- microRNA
- estrogen receptor
- miR-1290

Endocrine-Related Cancer (2013) **20**, 91–102

Introduction

There are large-scale molecular differences between estrogen receptor α (ERα)-positive and ER-negative breast cancers (Sorlie *et al.* 2003). ER is essential for estrogen-dependent growth, and its level of expression is a crucial determinant of response to endocrine therapy and prognosis in ER-positive breast cancer (Harvey *et al.* 1999, Yamashita *et al.* 2006, Dowsett *et al.* 2008). Recent analyses have identified heterogeneity in ER-positive

http://erc.endocrinology-journals.org
DOI: 10.1530/ERC-12-0207

Published by Bioscientifica Ltd.

breast cancer. Subtypes, named luminal A and luminal B, have been defined according to expression levels of Ki67, and the characteristics of these two subtypes are different (Goldhirsch *et al.* 2011). There is no doubt that higher concentrations of ER in the tumor cells are associated with a greater likelihood of a favorable response to endocrine therapy. However, little is known about how the expression of ER in breast cancer cells is regulated and how the biological characteristics of ER-positive breast cancer are determined. We recently analyzed expressions of microRNAs (miRNAs) that directly target ER in breast cancer. We found that miR-206 and miR-18a were downregulated in ER-positive breast cancer compared with ER-negative tumors and that low miR-18b expression was significantly associated with improved survival in HER2-negative breast cancer, although miR-18b expression was not correlated with ER protein expression (Kondo *et al.* 2008, Yoshimoto *et al.* 2011).

miRNAs are small (~21 nucleotides) noncoding RNAs that negatively regulate target genes by predominantly binding to the 3′-untranslated region (3′-UTR) of target mRNA, resulting in either mRNA degradation or translational repression (Krol *et al.* 2010). Recent studies have shown that miRNA mutations or dysregulated expression were associated with various human cancers and indicated that miRNAs can function as tumor suppressor genes and oncogenes (Esquela-Kerscher & Slack 2006). Expression profiling also revealed that miRNAs are differently expressed among molecular subtypes of breast cancer (Iorio *et al.* 2005). Significant associations were found between miRNA expression profiles and clinicopathological factors such as ER status and tumor grade (Blenkiron *et al.* 2007). Furthermore, recent studies have demonstrated that loss- or gain-of-function of specific miRNAs contributes to breast epithelial cellular transformation, tumorigenesis, and epithelial–mesenchymal transition and metastasis (Zhang & Ma 2012).

In this study, expression profiles of miRNAs and mRNAs in ER-positive breast cancer tissue were compared between ER^{high} $Ki67^{low}$ tumors and ER^{low} $Ki67^{high}$ tumors by miRNA and mRNA microarrays. Unsupervised hierarchical clustering analyses revealed distinct expression patterns of miRNAs and mRNAs in these two groups. We demonstrated that miR-1290 was downregulated and that six miRNAs were upregulated in ER^{high} $Ki67^{low}$ tumors. Protein expression patterns of the predicted target genes and the genes that were identified by mRNA expression profiling were analyzed in ER-positive breast cancer samples by immunohistochemistry (IHC). We identified miR-1290 and its potential target genes, forkhead box A1 (*FOXA1*) and *N*-acetyltransferase-1 (*NAT1*), being associated with characteristics of ER-positive breast cancer.

Materials and methods

Patients and breast cancer tissue

Breast tumor specimens from female patients with invasive breast carcinoma who were treated at Nagoya City University Hospital between 1995 and 2010 were included in the study (Table 1). The study protocol was approved by the institutional review board and conformed to the guidelines of the 1996 Declaration of Helsinki. Written informed consent for the use of surgically resected tumor tissues was provided by all patients before treatments. The samples were chosen from a continuous series of invasive carcinoma. All patients except those with stage IV disease underwent surgical treatment (mastectomy or lumpectomy). Tumor samples of patients with stage IV disease were taken by core needle biopsy. Patients received adequate endocrine or chemotherapy for adjuvant or metastatic diseases.

Microarray profiling of miRNA and mRNA expression

Total RNA was extracted from eight frozen samples of breast cancer tissue (Table 1). Extracted total RNA was labeled with Hy5 using the miRCURY LNA Array miR labeling kit (Exiqon, Vedbaek, Denmark). Labeled RNAs were hybridized onto 3D-Gene Human miRNA Oligo chips containing 1011 antisense probes printed in duplicate spots (Toray, Kamakura, Japan). The annotation and oligonucleotide sequences of the probes were conformed to the miRBase miRNA data base (http://microrna.sanger.ac.uk/sequences/). After stringent washes, fluorescent signals were scanned with the ScanArray Express Scanner (PerkinElmer, Waltham, MA, USA) and analyzed using GenePix Pro version 5.0 (Molecular Devices, Sunnyvale, CA, USA). These raw data of each spot were normalized by substitution with the mean intensity of the background signal determined by all blank spots' signal intensities at 95% confidence intervals. Measurements of both duplicate spots with signal intensities >2 S.D. of the background signal intensity were considered to be valid. A relative expression level of a given miRNA was calculated by comparing the signal intensities of the averaged valid spots with their mean value throughout the microarray experiments after normalization by their median values adjusted equivalently. miRNAs differentially expressed

http://erc.endocrinology-journals.org
DOI: 10.1530/ERC-12-0207

Published by Bioscientifica Ltd.

among the ER^{high} $Ki67^{low}$ tumors and ER^{low} $Ki67^{high}$ tumors were statistically identified using the Student's *t*-test and unsupervised hierarchical clustering analyses. Hierarchical clustering was performed with average linkage and Pearson's correlation. Differential expression was assessed by a nonparametric Wilcoxon's rank sum test for comparison between two groups. A heat-map was constructed by hierarchical clustering analysis using Cluster 2.0 Software (Tokyo, Japan) and the results were displayed with the TreeView program (http://rana.lbl.gov/eisen/). miRNA expression data are available from the National Center for Biotechnology Gene Expression Omnibus (GEO) at accession number (GEO:GSE38280).

mRNA expression profiles were examined using the same frozen breast cancer tissue samples as those used in miRNA analyses. Extracted total RNA was labeled with Cy5 using the Amino Allyl MessageAMP II aRNA Amplification kit (Applied Biosystems). Labeled RNAs were hybridized onto 3D-Gene Human mRNA Oligo chips 25k (Toray) was used (25 370 distinct genes). Hybridization signals were scanned and detected by the same method as that used in miRNA analyses. The gene expression data are available from GEO at accession number (GEO:GSE38280).

Quantitative RT-PCR detection of miRNAs

Total RNA was extracted from ~500 mg frozen breast cancer tissue using TRIzol reagent (Life Technologies, Inc.) as described previously (Kondo *et al.* 2008). cDNA was reverse transcribed from total RNA samples using specific miRNA primers from the TaqMan MicroRNA Assays and reagents from the TaqMan MicroRNA RT Kit (Applied Biosystems). The resulting cDNA was amplified by PCR using TaqMan MicroRNA Assay primers with the TaqMan Universal PCR Master Mix and analyzed with a 7300 ABI PRISM Sequence Detector System according to the manufacturer's instructions (Applied Biosystems). The relative levels of miRNA expression were calculated from the relevant signals by normalization with the signal for *U6B* miRNA expression. The assay names for each miRNA were as follows: hsa-let-7a for let-7a, hsa-miR-10a for miR-10a, hsa-miR-10b for miR-10b, hsa-miR-15a for 15a, hsa-miR-18a for miR-18a, hsa-miR-26a for miR-26a, hsa-miR-29c for miR-29c, hsa-miR-34a for miR-34a, hsa-miR-129 for miR-129, hsa-miR-146a for miR-146a, hsa-miR-193b for miR-193b, hsa-miR-342-3p for miR-342-3p, hsa-miR-1290 for miR-1290, and RNU6B for U6B miRNA (Applied Biosystems).

Immunohistochemistry

Tissue microarrays were constructed using paraffin-embedded, formalin-fixed tissue from 256 ER-positive breast cancer samples, including 64 samples from patients whose frozen samples were used in miRNA expression analysis. Tissue array sections were immunostained with 15 commercially available antibodies using the Bond-Max Autostainer (Leica Microsystems, Newcastle, UK) and the associated Bond Refine Polymer Detection Kit (Yamashita *et al.* 2006). Details of primary antibodies and scoring manners are described in Supplementary Table 1, see section on supplementary data given at the end of this article. HER2-positive tumors were excluded from this study.

Cell culture and transfections

MCF-7 cells (American Type Culture Collection (ATCC), Manassas, VA, USA) were grown in RPMI 1640 medium containing 10% fetal bovine serum (FBS), 2 mmol/l L-glutamine and penicillin–streptomycin (50 IU/ml and 50 mg/ml respectively), and 0.1% human insulin at 37 °C with 5% CO_2. T47D cells (ATCC) were grown in RPMI 1640 medium containing 10% FBS and 2 mmol/l L-glutamine and penicillin–streptomycin (50 IU/ml and 50 mg/ml respectively) at 37 °C with 5% CO_2. Transfections of pre-miR-1290 precursor (hsa-miR-1290; Ambion, Inc., Austin, TX, USA) were performed with Cell Line Nucleofector kits (Amaxa Biosystems, Cologne, Germany) using a Nucleofector device (Amaxa Biosystems) according to the manufacturer's instructions (Kondo *et al.* 2008). A nonspecific control miRNA (Pre-miR miRNA Inhibitors-Negative Control #1; Ambion, Inc.) was used as a negative control.

Quantitative RT-PCR detection of miR-1290 and mRNAs

Total RNA was extracted from 2×10^6 cells with miRNeasy Mini Kit (Qiagen) using a QIAcube (Qiagen) according to the manufacturer's instructions. cDNA was reverse transcribed using specific miRNA primers and the relative levels of miR-1290 expression were measured as described earlier. Total RNA (1 μg) was also subjected to RT with random primers in a 20 μl reaction volume using High-Capacity cDNA RT Kit (Applied Biosystems). mRNA expression was measured by quantitative RT-PCR with the TaqMan Universal PCR Master Mix using a 7500 ABI PRISM Sequence Detector System according to the manufacturer's instructions (Applied Biosystems; Kondo *et al.* 2008). The relative levels of mRNA expression were

http://erc.endocrinology-journals.org
DOI: 10.1530/ERC-12-0207

Published by Bioscientifica Ltd.

Table 1 Clinicopathological characteristics of patients and breast tumors with ER-positive, HER2-negative breast cancer.

	Samples for miRNA and mRNA microarray analyses		Samples for miRNA quantitative RT-PCR analysis	Samples for immunohistochemistry
	ER^{high} $Ki67^{low}$	ER^{low} $Ki67^{high}$	Total	Total
No. of patients	4	4	64	256
Age (years)				
Mean±S.D.	71.8±20.9	57.5±12.1	60.0±12.0	58.0±13.0
Range	44–91	42–69	32–88	28–91
Tumor size (cm)				
Mean±S.D.	1.5±0.4	1.6±0.7		
≤2.0			20 (31%)	148 (57.9%)
2.1–5.0			38 (59%)	102 (39.8%)
>5.0			6 (10%)	6 (2.3%)
No. of positive lymph nodes				
0	4 (100%)	4 (100%)	34 (53%)	135 (52.7%)
1–3	0 (0%)	0 (0%)	16 (25%)	72 (28.1%)
4–9	0 (0%)	0 (0%)	6 (10%)	11 (4.3%)
≥10	0 (0%)	0 (0%)	4 (6%)	7 (2.7%)
Unknown	0 (0%)	0 (0%)	4 (6%)	31 (12.2%)
Tumor grade				
1	4 (100%)	0 (0%)	16 (25%)	95 (37.1%)
2	0 (0%)	0 (0%)	36 (56%)	69 (27.0%)
3	0 (0%)	4 (100%)	12 (19%)	92 (35.9%)
ER (Allred score)				
Mean±S.D.	7.8±0.5	3.5±0.6		
0–2 (negative)			0 (0%)	0 (0%)
3–8 (positive)			64 (100%)	256 (100%)
PgR (Allred score)				
Mean±S.D.	7.8±0.5	2.5±0.6		
0–2 (negative)			10 (16%)	34 (13.3%)
3–8 (positive)			54 (84%)	222 (86.7%)
HER2 status				
Negative	4 (100%)	4 (100%)	64 (100%)	256 (100%)
Positive	0 (0%)	0 (0%)	0 (0%)	0 (0%)
Ki67 (labeling index, %)				
Mean±S.D.	6.1±2.7	50.8±11.8		
Adjuvant therapy				
None			8	27
Endocrine therapy			32	127
Chemotherapy			3	4
Combined			21	98

calculated from the relevant signals by normalization with the signal for β-actin mRNA expression. The assay numbers for BCL2, FOXA1, microtubule-associated protein tau (MAPT), NAT1, and β-actin were as follows: Hs00608023_m1 for BCL2, Hs00270129_m1 for FOXA1, Hs00902314_m1 for MAPT, Hs00265080_m1 for NAT1, and 4333762T for β-actin (Applied Biosystems).

Western blotting

Cells were pelleted by centrifugation and solubilized in lysis buffer containing protease inhibitor and phosphatase inhibitor cocktails (Thermo Scientific, Yokohama, Japan). Equal amounts of total protein (30 μg) from whole cell lysates were prepared and electrophoresed on 12% (w/v) SDS–polyacrylamide gels (NuPAGE Bis–Tris Gel, Invitrogen) transferred to polyvinylidene difluoride membranes (Invitrogen) and immunoblotted using specific antibodies (Supplementary Table 1; Yamashita *et al.* 2003). Anti-mouse or anti-rabbit IgG, HRP-linked Whole Antibodies (GE Healthcare Japan, Tokyo, Japan) were used as secondary antibodies at 1:10 000 dilution. Antibody binding was visualized with ECL Western Blotting Detection System (GE Healthcare Japan) using Light-Capture AE-6981 (ATTO, Tokyo, Japan) according to the manufacturer's instructions. Image J Software from the National Institutes of Health (Bethesda, MD, USA) was used to quantify band intensities.

http://erc.endocrinology-journals.org
DOI: 10.1530/ERC-12-0207

Published by Bioscientifica Ltd.

Statistical analysis

Spearman's rank correlation test was used to study relationships between expression levels of miRNAs and clinicopathological factors, expression levels of proteins and clinicopathological factors, expression levels of miRNAs and proteins, and expression levels of miRNAs and mRNAs. $P<0.05$ is considered significant in Spearman's rank correlation test.

Results

Differentially expressed miRNAs in ER^{high} $Ki67^{low}$ tumors and ER^{low} $Ki67^{high}$ tumors in breast cancer tissue

Expression profiles of miRNAs and mRNAs in ER-positive breast cancer tissue were compared between ER^{high} $Ki67^{low}$ tumors and ER^{low} $Ki67^{high}$ tumors by miRNA and mRNA microarrays using eight frozen samples of breast cancer tissue (four tumors in each group; Table 1). Unsupervised hierarchical clustering analyses revealed 67 miRNAs in 1011 miRNAs and 657 mRNAs in 25 370 mRNAs that were differentially expressed in ER^{high} $Ki67^{low}$ tumors and ER^{low} $Ki67^{high}$ tumors ($P<0.01$; Supplementary Figure 1, see section on supplementary data given at the end of this article and Supplementary Table 2, see section on supplementary data given at the end of this article, and $P<0.01$; Supplementary Figure 2, see section on supplementary data given at the end of this article and Supplementary Tables 3 and 4, see section on supplementary data given at the end of this article respectively). We selected 12 miRNAs (let-7a, miR-10a, miR-10b, miR-15a, miR-26a, miR-29c, miR-34a, miR-129, miR-146a, miR-193b, miR-342-3p, and miR-1290) that were differentially expressed in these two groups. Among differentially expressed 67 miRNAs, the above 12 miRNAs, especially let-7a, miR-10a, miR-10b, miR-15a, miR-26a, miR-29c, miR-34a, miR-146a, and miR-342-3p, have been reported to be related to breast cancer development and carcinogenesis (Mattie *et al.* 2006, Blenkiron *et al.* 2007, O'Day & Lal 2010). miR-193b has been reported to be related to ERα (Yoshimoto *et al.* 2011). Moreover, we referred to the reported mRNA microarray analyses to classify luminal A and luminal B subtypes in order to select key genes (Sorlie *et al.* 2003, Parker *et al.* 2009), including *FOXA1*, *NAT1*, *MAPT*, *XBP1*, and *BCL2*, which have target sequences in the 3′-UTR regions of 67 differentially expressed miRNAs according to *in silico* analysis using TargetScan, PicTar, and MiRanda, and selected miR-146a and miR-1290, which were downregulated in ER^{high} $Ki67^{low}$ tumors. Quantitative RT-PCR detection analysis using 64 frozen breast cancer tissue samples (Table 2 and Supplementary Table 5, see section on supplementary data given at the end of this article) identified six miRNAs (let-7a, miR-15a, miR-26a, miR-34a, miR-193b, and miR-342-3p) that were upregulated in ER^{high} tumors ($P=0.0002$, $P=0.0006$, $P=0.0082$, $P<0.0001$, $P=0.0142$, and $P=0.0002$ respectively; Table 3). miR-1290 was also included in further analyses because it was the only miRNA among the selected miRNAs that was downregulated in ER^{high} $Ki67^{low}$ tumors and its expression levels were strongly correlated with tumor grade ($P<0.0001$; Table 3).

Table 2 Expression levels of 12 selected miRNAs and the control miRNA (U6B) in 64 ER-positive breast cancer tissues by quantitative RT-PCR analysis.

	Mean ± S.E.M.
let-7a	22.079 ± 0.173
miR-10a	26.585 ± 0.278
miR-10b	27.636 ± 0.247
miR-15a	27.100 ± 0.285
miR-26a	22.711 ± 0.201
miR-29c	24.295 ± 0.390
miR-34a	26.339 ± 0.240
mR-129	34.759 ± 0.185
miR-146a	26.160 ± 0.221
miR-193b	21.112 ± 0.219
miR-342-3p	24.456 ± 0.322
miR-1290	27.612 ± 0.445
U6B	27.091 ± 0.154

The potential target genes for seven selected miRNAs (let-7a, miR-15a, miR-26a, miR-34a, miR-193b, miR-342-3p, and miR-1290) were predicted according to *in silico* analysis using TargetScan, PicTar, and MiRanda. In addition, 657 mRNAs that were differentially expressed in ER^{high} $Ki67^{low}$ tumors and ER^{low} $Ki67^{high}$ tumors in microarray analysis were considered to select putative target genes. Finally, we picked up 11 proteins (ANKRD30, BCL2, cyclin D1, FOXA1, GATA3, LIN28, MAPT, NAT1, RB1, P53 (TP53), and XBP1) that were products of potential target genes for seven selected miRNAs and that were considered to be differentially expressed in ER^{high} $Ki67^{low}$ tumors and ER^{low} $Ki67^{high}$ tumors (Table 4). *ANKRD30* was the most differentially expressed gene between ER^{high} $Ki67^{low}$ tumors and ER^{low} $Ki67^{high}$ tumors. BCL2, cyclin D1, LIN28, and RB1 are potential targets of the selected miRNAs as shown in Table 4. FOXA1, GATA3, NAT1, and XBP1 were strongly downregulated in ER^{low} $Ki67^{high}$ tumors, putative targets of the selected miRNAs, and reported as to be related with ER-positive breast

http://erc.endocrinology-journals.org
DOI: 10.1530/ERC-12-0207

Published by Bioscientifica Ltd.

Table 3 Correlation between expression levels of miRNAs and clinicopathological factors ($n=64$).

	ER	PgR	Tumor grade	Ki67	Tumor size	No. of positive lymph nodes
let-7a	+0.533[a] 0.0002*,[b]	+0.349 0.0087*	−0.033 0.2536	−0.115 0.3717	−0.068 0.5854	+0.123 0.7959
miR-10a	+0.286 0.1114	+0.219 0.1113	+0.005 0.4012	−0.113 0.3757	−0.326 0.0098*	+0.132 0.7399
miR-10b	+0.268 0.1646	+0.130 0.3894	+0.074 0.8411	−0.114 0.375	−0.185 0.1439	+0.171 0.5025
miR-15a	+0.499 0.0006*	+0.081 0.6396	+0.215 0.3036	+0.055 0.6729	−0.129 0.3084	+0.062 0.7917
miR-26a	+0.414 0.0082*	+0.165 0.2585	+0.065 0.7953	−0.056 0.6674	−0.003 0.9712	+0.060 0.8038
miR-29c	+0.206 0.3839	−0.030 0.6671	+0.115 0.8782	+0.018 0.8917	−0.084 0.5117	+0.121 0.7546
miR-34a	+0.785 <0.0001*	+0.164 0.2558	+0.061 0.7535	+0.034 0.7941	−0.168 0.1851	+0.039 0.6458
mR-129	+0.334 0.0528	+0.043 0.8722	+0.334 0.0384*	−0.056 0.6711	−0.006 0.9746	+0.049 0.677
miR-146a	+0.101 0.9032	−0.149 0.1819	+0.425 0.0073*	+0.007 0.9586	−0.052 0.6966	−0.009 0.5031
miR-193b	+0.387 0.0142*	+0.203 0.1483	+0.223 0.2666	+0.078 0.5493	+0.046 0.7298	+0.214 0.2889
miR-342-3p	+0.539 0.0002*	+0.131 0.3975	+0.131 0.8024	−0.039 0.7657	−0.016 0.8932	+0.107 0.9081
miR-1290	+0.014 0.3987	−0.211 0.0581	+0.585 <0.0001*	+0.228 0.0748	+0.029 0.8267	+0.280 0.1109

*$P<0.05$ is considered significant.
[a]Spearman's correlation coefficient.
[b]P, Spearman's rank correlation test.

cancer. MAPT is also reported to be related with ER-positive breast cancer and a potential target of miR-1290. P53 was selected as a target of let-7a.

Expression of the potential target genes in ER-positive, HER2-negative breast cancer

We examined protein expression of 11 selected target genes in ER-positive, HER2-negative breast cancer by IHC (Supplementary Table 6, see section on supplementary data given at the end of this article). Expression levels of BCL2, FOXA1, GATA3, LIN28, MAPT, and NAT1 were positively correlated with expression levels of ER ($P<0.0001$, $P<0.0001$, $P<0.0001$, $P=0.0008$, $P<0.0001$, and $P=0.0005$ respectively; Table 4). Expression levels of ANKRD30, BCL2, FOXA1, GATA3, LIN28, MAPT, and NAT1 were positively correlated with expression levels of progesterone receptor (PgR; $P=0.0246$, $P=0.0059$, $P=0.0005$, $P<0.0001$, $P=0.017$, $P<0.0001$, and $P<0.0001$ respectively). Expression levels of ANKRD30, BCL2, and TP53 were positively correlated with tumor grade ($P=0.0012$, $P=0.0109$, and $P=0.0108$ respectively), whereas expression levels of CCND1, FOXA1, GATA3, LIN28, MAPT, NAT1, and XBP1 were negatively correlated with tumor grade ($P=0.0101$, $P<0.0001$, $P<0.0001$, $P=0.0099$, $P<0.0001$, $P<0.0001$, and $P=0.0018$ respectively). Expression levels of LIN28 and TP53 were positively correlated with expression levels of Ki67 ($P=0.0446$ and $P=0.002$ respectively), while expression levels of MAPT and NAT1 were negatively correlated with expression levels of Ki67 ($P=0.0419$ and $P=0.0095$ respectively). Expression levels of ANKRD30, FOXA1, GATA3, LIN28, MAPT, NAT1, TP53, and XBP1 were negatively correlated with tumor size ($P<0.0001$, $P=0.0009$, $P=0.0001$, $P<0.0001$, $P=0.0093$, $P=0.0004$, $P=0.0336$, and $P=0.0203$ respectively). There was no association between expression of 11 selected proteins and lymph node status (Table 4).

We then compared expression levels of seven selected miRNAs (let-7a, miR-15a, miR-26a, miR-34a, miR-193b, miR-342-3p, and miR-1290) and their potential target genes (*ANKRD30*, *BCL2*, cyclin D1, *FOXA1*, *GATA3*, *LIN28*, *MAPT*, *NAT1*, *RB1*, *P53*, and *XBP1*) using 64 samples of breast cancer tissue, simultaneously analyzing miRNA expression by quantitative RT-PCR and protein expression by IHC. Interestingly, expression levels of miR-1290 were

http://erc.endocrinology-journals.org
DOI: 10.1530/ERC-12-0207

Published by Bioscientifica Ltd.

Table 4 Correlation between expression levels of potential target proteins and clinicopathological factors ($n=256$).

	ER	PgR	Tumor grade	Ki67	Tumor size	No. of positive lymph nodes	miRNAs
ANKRD30	+0.260[a] 0.2265[b]	+0.250 0.0246*	+0.002 0.0012*	+0.142 0.5865	−0.145 <0.0001*	+0.176 0.2769	miR-193b
BCL2	+0.467 <0.0001*	+0.320 0.0059*	+0.102 0.0109*	+0.132 0.4585	+0.078 0.0968	+0.278 0.8608	let-7a, miR-10a, miR-15a, miR-26a, miR-29c, miR-34a, miR-1290
CCND1	+0.177 0.5364	+0.083 0.6216	−0.190 0.0101*	+0.078 0.5415	−0.085 0.4981	+0.046 0.6898	miR-15a, miR-34a, miR-193b
FOXA1	+0.407 <0.0001*	+0.234 0.0005*	−0.235 <0.0001*	−0.082 0.1939	−0.210 0.0009*	+0.009 0.103	miR-129, miR-1290
GATA3	+0.448 <0.0001*	+0.286 <0.0001*	−0.224 <0.0001*	−0.004 0.9441	−0.242 0.0001*	−0.005 0.0655	miR-10a, miR-10b, miR-34a
LIN28	+0.289 0.0008*	+0.173 0.017*	−0.081 0.0099*	+0.138 0.0446*	−0.238 <0.0001*	+0.068 0.3681	let-7a, miR-26a, miR-34a, miR-129, miR-342-3p
MAPT	+0.356 <0.0001*	0.494 <0.0001*	−0.254 <0.0001*	−0.144 0.0419*	−0.149 0.0093*	+0.030 0.1314	miR-34a, miR-1290
NAT1	+0.316 0.0005*	+0.394 <0.0001*	−0.274 <0.0001*	−0.122 0.0095*	−0.180 0.0004*	+0.105 0.4956	miR-1290
RB1	+0.248 0.0751	+0.261 0.8369	+0.327 0.4651	+0.290 0.2424	+0.263 0.6956	+0.374 0.6748	let-7a, miR-26a, miR-34a, miR-129, miR-1290
TP53	−0.016 0.0743	−0.010 0.6815	+0.211 0.0108*	+0.197 0.002*	−0.133 0.0336*	+0.074 0.5783	let-7a
XBP1	+0.183 0.5653	−0.042 0.5318	−0.236 0.0018*	+0.079 0.5906	−0.278 0.0203*	−0.040 0.2069	miR-34a

*$P<0.05$ is considered significant.
[a]Spearman's correlation coefficient.
[b]P, Spearman's rank correlation test.

inversely correlated with expression levels of *BCL2*, *FOXA1*, *MAPT*, and *NAT1*, all of which are predictive targets of miR-1290 according to *in silico* analysis ($P=0.020$, $P=0.044$, $P=0.040$, and $P=0.0098$ respectively; Fig. 1A, B, C and D), suggesting that miR-1290 might downregulate these four genes in ER-positive breast cancer. Moreover, let-7a expression was inversely correlated with P53 expression ($P=0.038$; Fig. 1E). No association was found between other miRNA expressions and their putative target gene expressions.

miR-1290 downregulates FOXA1 and NAT1 in ER-positive breast cancer cells

We extended our analysis to clarify whether miR-1290 downregulates BCL2, FOXA1, MAPT, and NAT1 in ER-positive breast cancer cells. Pre-miR-1290 precursor was introduced into T47D and MCF-7 cells. Cells were transfected with either control miRNA (300 nmol/l) or pre-miR-1290 precursor at various concentrations (10–300 nmol/l) and incubated for 24 h in T47D cells and for 36 h in MCF-7 cells. Expression levels of miR-1290 and mRNA expression levels of *BCL2*, *FOXA1*, *MAPT*, and *NAT1* were quantitatively measured using parallel samples. Transfection with pre-miR-1290 produced a dose-dependent increase in miR-1290 expression levels (Fig. 2A, left), whereas expression levels of miR-1290 were inversely correlated with expression levels of *FOXA1* ($P=0.0003$; Fig. 2A, top right) and *NAT1* ($P<0.0001$; Fig. 2A, bottom right) mRNAs, but not with *BCL2* or *MAPT* mRNA, in T47D cells (Fig. 2A). Moreover, expression levels of miR-1290 were inversely correlated with expression levels of *NAT1* mRNA ($P=0.037$; Fig. 2B, bottom right), but not with *BCL2*, *FOXA1*, or *MAPT* mRNA, in MCF-7 cells (Fig. 2B).

The effects of miR-1290 on protein expression of BCL2, FOXA1, MAPT, and NAT1 were examined in T47D and MCF-7 cells by western blot analysis. When T47D cells were transfected with either control miRNA (300 nmol/l) or pre-miR-1290 precursor at various concentrations (30–1000 nmol/l) and incubated for 48 h, miR-1290 induced a dose-dependent decrease in protein expression of NAT1, reducing it ~60%, but not BCL2, FOXA1, or MAPT (Fig. 2C). Effects of miR-1290 on protein expression of BCL2, FOXA1, MAPT, and NAT1 were not clear in MCF-7 cells (Fig. 2D). From these analyses, we conclude that miR-1290 might downregulate FOXA1 and NAT1 in ER-positive breast cancer cells.

http://erc.endocrinology-journals.org
DOI: 10.1530/ERC-12-0207

Published by Bioscientifica Ltd.

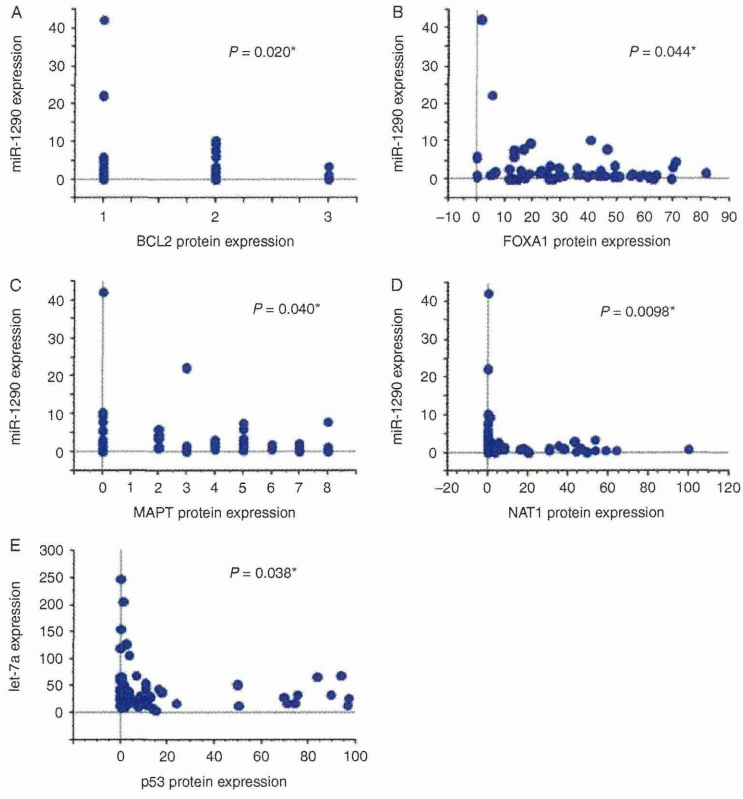

Figure 1

miR-1290 expression is inversely correlated with expressions of BCL2, FOXA1, MAPT, and NAT1. Scatter plots show inverse correlations between miR-1290 and BCL2 (A), FOXA1 (B), MAPT (C), and NAT1 (D) protein expression in breast cancer tissue ($P=0.020$, $P=0.044$, $P=0.040$, and $P=0.0098$ respectively). (E) let-7 expression is inversely correlated with P53 protein expression in breast cancer tissue ($P=0.038$).

Discussion

In this study, we have shown distinct expression patterns of miRNAs and mRNAs in luminal A and luminal B subtypes in ER-positive breast cancer. We demonstrated that miR-1290 and its potential target genes, *FOXA1* and *NAT1*, might be associated with characteristics of ER-positive disease. miR-1290 expression was strongly downregulated in ER^{high} $Ki67^{low}$ tumors and was positively correlated with tumor grade. Although the role of miR-1290 has not been analyzed as yet, it was reported that 36 miRNAs, including miR-1290, were circulating at increased levels in patients with renal cell carcinoma and were overexpressed in corresponding renal cell carcinoma tissue (Wulfken *et al.* 2011). It was also reported that six miRNAs, including miR-1290, were upregulated in drug-sensitive cells following Y-Box protein 1 inhibition, but no differences in miRNA expression could be detected in multidrug-resistant gastric carcinoma cells (Belian *et al.* 2010).

FOXA1, a forkhead family transcription factor, has been reported to be expressed predominantly in luminal A breast cancer with favorable prognosis (Badve *et al.* 2007, Mehta *et al.* 2012). Hurtado *et al.* recently reported that FOXA1 creates an open conformation at ER-binding sites and that ER can bind and activate target gene expression in the presence of estrogen. Thus, FOXA1 is a key determinant of ER function and endocrine response in breast cancer (Hurtado *et al.* 2011). They also reported that the differential ER-binding program observed in tumors from patients with poor outcome is due to the FOXA1-mediated reprogramming of ER binding (Ross-Innes *et al.* 2012). We demonstrated that FOXA1 expression is much higher in ER^{high} $Ki67^{low}$ tumors than in ER^{low} $Ki67^{high}$ tumors and that expression levels of FOXA1 were strongly and positively correlated with expression levels of ER and

http://erc.endocrinology-journals.org
DOI: 10.1530/ERC-12-0207

Published by Bioscientifica Ltd.

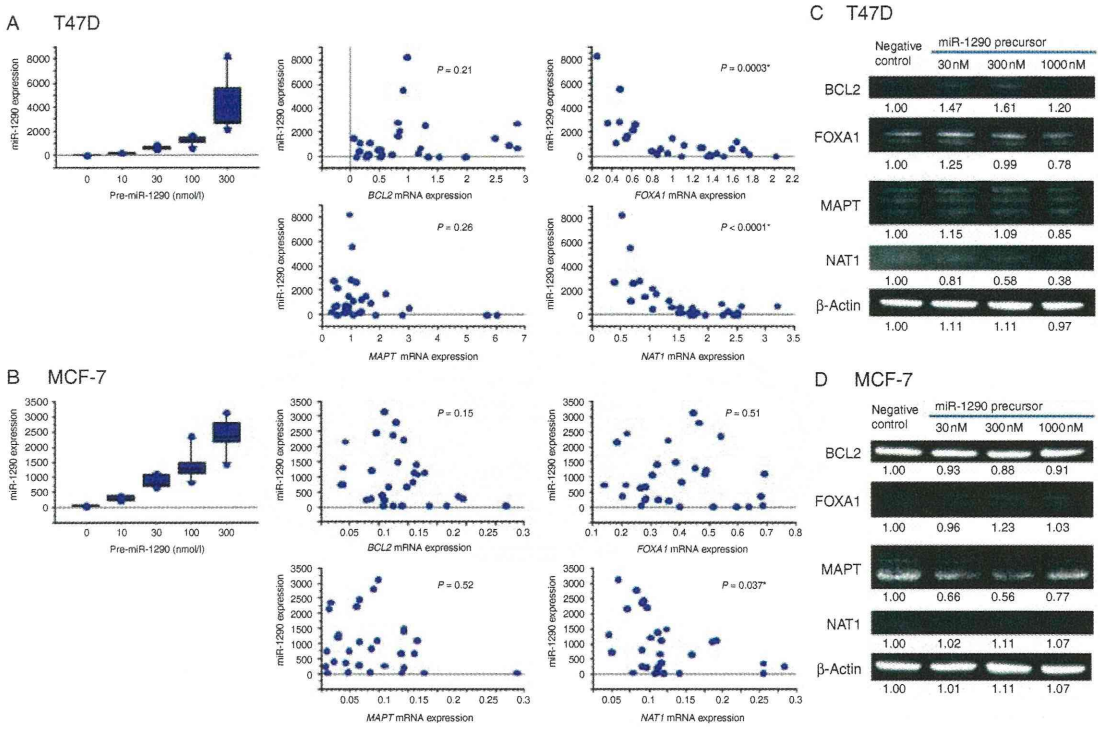

Figure 2

Gene expressions of miR-1290 putative targets in T47D and MCF-7 cells transfected with miR-1290. (A) T47D cells were transfected with either control miRNA (300 nmol/l) or pre-miR-1290 precursor at 10–300 nmol/l and incubated for 24 h. Expression levels of miR-1290 and mRNA levels of BCL2, FOXA1, MAPT, and NAT1 were measured by quantitative RT-PCR. Scatter plots show inverse correlation between miR-1290 expression and *FOXA1* and *NAT1* mRNA expression ($P=0.0003$ and $P<0.0001$ respectively). (B) MCF-7 cells were transfected with either control miRNA (300 nmol/l) or pre-miR-1290 precursor at 10–300 nmol/l and incubated for 36 h. Expression levels of miR-1290 and mRNA levels of BCL2, FOXA1, MAPT, and NAT1 were measured by quantitative RT-PCR. Scatter plots show inverse correlation between miR-1290 expression and *NAT1* mRNA expression ($P=0.037$). (C) T47D cells were transfected with either control miRNA (300 nmol/l) or pre-miR-1290 precursor at 30–1000 nmol/l and incubated for 48 h. Protein expression of BCL2, FOXA1, MAPT, and NAT1 was assayed by western blot analysis. The number below the band represents the mean value from densitometry reading, relative to the negative control, which was set at 1.00. Representative results from one of the three experiments are shown. (D) MCF-7 cells were transfected with either control miRNA (300 nmol/l) or pre-miR-1290 precursor at 30–1000 nmol/l and incubated for 48 h. Protein expression of BCL2, FOXA1, MAPT, and NAT1 was assayed by western blot analysis. The number below the band represents the mean value from densitometry reading, relative to the negative control, which was set at 1.00. Representative results from one of the three experiments are shown.

PgR and negatively associated with tumor grade in ER-positive breast cancer. Moreover, introduction of miR-1290 into estrogen-dependent breast cancer cells reduced FOXA1 expression. Because FOXA1 is a putative target of miR-1290 according to *in silico* analysis, we suggest that miR-1290 is a key factor for regulating FOXA1, which is associated with characteristics of ER-positive breast cancer.

Arylamine NATs, known as drug- and carcinogen-metabolizing enzymes, transfer an acetyl group from acetyl coenzyme A to arylamines (Sim *et al.* 2008). Several studies have shown higher mRNA and protein expression of NAT1 in ER-positive breast cancer compared with the expression in ER-negative disease (Perou *et al.* 2000, Adam *et al.* 2003, Tozlu *et al.* 2006, Wakefield *et al.* 2008). Moreover, it was reported that high expression of NAT1 was correlated with better outcome in ER-positive breast cancer (Bieche *et al.* 2004, Dolled-Filhart *et al.* 2006). Our results demonstrated that *NAT1* mRNA expression was much higher in ER^{high} $Ki67^{low}$ tumors than in ER^{low} $Ki67^{high}$ tumors by microarray analyses and that NAT1 protein expression by IHC showed positive correlation with expression levels of ER and PgR and negative correlation with expression levels of Ki67, tumor grade, and tumor size. In addition, introduction of miR-1290 into estrogen-dependent breast cancer cells strongly

http://erc.endocrinology-journals.org
DOI: 10.1530/ERC-12-0207

Published by Bioscientifica Ltd.